

# **Monitoring anthropogenic metal released in the environment via X-ray fluorescence, absorption and diffraction at micrometer scales of resolution**

A. Manceau<sup>1,2</sup>, M.A. Marcus<sup>1</sup>, N. Tamura<sup>1</sup>, R.S. Celestre<sup>1</sup>, A.A. MacDowell<sup>1</sup>, R.E. Sublett<sup>1</sup>, H.A. Padmore<sup>1</sup>, M. Kersten<sup>3</sup>

<sup>1</sup>Advanced Light Source, Lawrence Berkeley National Laboratory, Berkeley, CA 94720

<sup>2</sup>Environmental Geochemistry Group, Hilgard Hall, University of California, Berkeley, CA 94720

<sup>3</sup>Geoscience Institute, Gutenberg University, 55099 Mainz, Germany

## **INTRODUCTION**

Ferromanganese nodules are common in aquatic systems, including lacustrine and shallow marine environments, and also on the oceanic seafloor. They generally have a banded structure consisting of practically pure and alternating Fe- and Mn-rich layers separated by mixed Fe-Mn zones. This concretion-like growth pattern is attributed to intermittent oxidizing and reducing conditions. Accretion of ferromanganese nodules may cover time scales up to millions of years. The implication that they provide a continuously growing substrate with constant sorption efficiency for trace elements is the basis of a resurging interest for Fe-Mn nodules focusing on their possible use as a paleoproxy record for long-term environmental changes. Therefore, an idea was born to try and assess the metal fluxes into the ferromanganese nodules by dating individual nodule growth layers, and to compare these fluxes with the temporal variability in anthropogenic emissions. The prerequisite for such an approach is high-resolution profiling due to the slow accretion of the nodule material. Synchrotron-based micro-X-ray fluorescence ( $\mu$ SXRF) was applied to obtain in-situ trace element profiles of the necessary spatial resolution, as a basis for the evaluation of nodule accretion rates and for an assessment of their use for retrospective monitoring of excess metal input in the western Baltic Sea. Then, in-situ X-ray diffraction (XRD) and extended X-ray absorption fine structure (EXAFS) spectroscopy at the Mn and Zn K-edge were performed at the micrometer resolution to determine how anthropogenic Zn is taken up.

## **EXPERIMENTS**

The examined nodule was collected in shallow water of the SW Baltic Sea where nodules are relatively fast-growing and enriched in metal contaminants, thus making them highly suitable to record the anthropogenic pollution in the last century. The sample was prepared as a micropolished 30  $\mu$ m-thick thin section. The  $\mu$ XRD patterns of Fe- and Mn-pure layers were recorded on Beamline 7.3.3., and  $\mu$ EXAFS spectra were collected on Beamline 10.3.2. In both experiments,  $\mu$ SXRF maps were first recorded to image the Fe and Mn layers. All experiments were conducted with a beamsize of 15 (H) x 5 to 10 (V)  $\mu$ m.

## **RESULTS AND INTERPRETATION**

The  $\mu$ SXRF element map of Fe and Mn (Fig. 1) shows the typically cusped zebra-type band structure of the Fe-Mn concretions. The thickness of Mn-rich layers varies typically from 200 to 500  $\mu$ m and that of the Fe-rich layers from about 100 to 200  $\mu$ m. Of the trace elements investigated (Co, Ni, Cu, and Zn), Zn showed the most significant enrichment, with values in the outermost surface Mn layers of up to six-fold higher than those found in older core parts. Thus, the high-resolution Zn profiles provide the necessary temporal resolution for a dating method

analogous to dendrochronology. Assuming a continuous accretion of these relatively fast growing nodules (on average  $20 \mu\text{m yr}^{-1}$ ) over the last century, the Zn enrichment was assessed to have commenced in 1880/90, reflecting the enhanced heavy metal emissions with rising industrialization in Europe.  $\mu\text{XRD}$  patterns collected in Fe-rich regions (Fig. 2) contain only a broad and faint double hump with maxima at about  $2.85 \text{ \AA}$  and  $2.25 \text{ \AA}$ . The centroid of this hump is at about  $2.5 \text{ \AA}$  as in poorly-crystallized two-line ferrihydrite (hydrous ferric oxide). Minor amounts of detrital quartz grains and silica particles (opal-A) were also detected by  $\mu\text{XRD}$ . The  $\mu\text{XRD}$  patterns taken in the Mn-rich layers look completely different consisting of a series of basal reflection peaks at  $7.07 \text{ \AA}$  (001),  $3.51 \text{ \AA}$  (002) and  $hk0$  peaks at  $2.46 \text{ \AA}$  (200) and  $1.43 \text{ \AA}$  (110). These peak positions, together with the noteworthy asymmetrical shape of the (200) reflection, are characteristic of turbostratic hexagonal birnessite ( $\delta\text{-MnO}_2$ ).

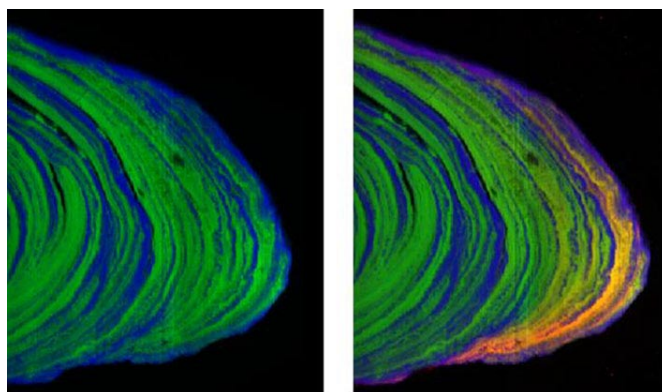


Figure 1. Synchrotron-based micro-X-ray radiation fluorescence ( $\mu\text{SXRF}$ ) Fe and Mn maps of the outermost Fe and Mn layers of a ferromanganese nodule from the Baltic sea ( $6600 \mu\text{m} \times 3780 \mu\text{m}$ , step size  $15 \mu\text{m}$ , counting time 250 ms/pixel, red = Zn, green = Mn, blue = Fe, beamline: 10.3.2.). The onion-like structure of growth rims is clearly discernible as few hundreds  $\mu\text{m}$  thick Fe/Mn-rich bandings. Zn is exclusively associated with Mn, as indicated by the orange color of the Zn-containing Mn layers, and its concentration increases towards the surface.

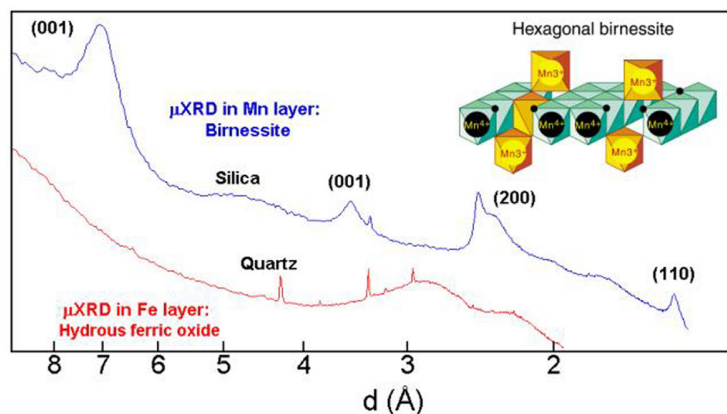


Figure 2. X-ray microdiffractograms collected in Mn ( $\lambda = 1.252 \text{ \AA}$ ) and Fe ( $\lambda = 1.758 \text{ \AA}$ ) layers. Mn is speciated as turbostratic hexagonal birnessite ( $\delta\text{-MnO}_2$ ), and Fe as hydrous ferric oxide. Quartz grains (sharp peaks) and silica particles ( $d \approx 4.6 \text{ \AA}$ ) were detected throughout the sample.

To determine the Zn sorption mechanism at the molecular-level, Zn K-edge  $\mu\text{EXAFS}$  spectra were collected in a Zn ‘hot spot’. Qualitative information about the local structure of Zn can be obtained by comparing the unknown  $\mu\text{EXAFS}$  spectrum to reference EXAFS spectra from relevant model

compounds. The best spectral match was obtained with the Zn-sorbed birnessite reference, in which Zn is predominantly tetrahedrally, and secondarily octahedrally, coordinated and complexed above vacant sites of the manganese layer (Fig. 3). Comparison of radial structure functions (Fig. 3b) indicates that the Zn-O and Zn-Mn distances are both slightly, but significantly, shortened in the nodule sample, which is indicative of the presence of only  $^{IV}\text{Zn}$ . The preferred formation of the  $^{IV}\text{Zn}$  over the  $^{VI}\text{Zn}$  complex presumably arises from the presence of aliovalent  $\text{Mn}^{3+}$  ions within the  $\text{MnO}_2$  layer, because 4-fold coordinated Zn provides more positive charges to undersaturated oxygens ( $2+/4 = 0.5$  v.u.) than a 6-fold coordinated Zn ( $2+/6 = 0.33$  v.u.).

## CONCLUSION

This study demonstrates the merit of deploying in parallel fluorescence, diffraction, and absorption studies at micrometer scales of resolution. This unprecedented combination of techniques allows the determination of the structural form of trace elements in heterogeneous matrices with an unequaled precision. Since much of nature and synthetic materials are heterogeneous on micron and sub-micron length scales, we anticipate that the synergistic use of  $\mu\text{SXRF}$ ,  $\mu\text{SXRD}$ , and  $\mu\text{EXAFS}$  will have broad applications and add to the arsenal of analytical methods available in environmental and materials science.

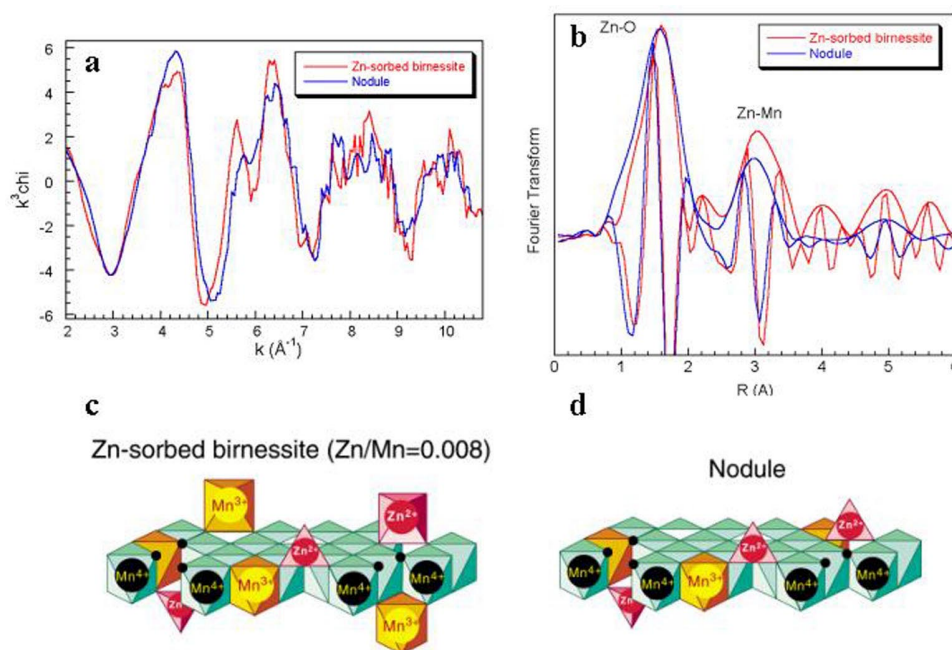


Figure 3. Zn K-edge  $\mu\text{EXAFS}$  spectrum and Fourier transform (modulus plus imaginary part) from a Zn ‘hot spot’ of the nodule rim presented in Fig. 1, compared to the Zn-edge data from a Zn-sorbed birnessite reference, in which Zn is sorbed as a mix of  $^{IV}\text{Zn}$  and  $^{VI}\text{Zn}$  complexes above vacant layer Mn sites. The unknown and reference data look similar, indicating that Zn are uptaken in a similar manner in the two compounds. However, Zn-O and Zn-Mn distances are clearly shorter in the natural sample because Zn is only four-fold coordinated.

This work was supported by the Director, Office of Energy Research, Office of Basic Energy Sciences, Materials Science Division, of the U.S. Department of Energy under Contract No. DE-AC03-76SF00098.

Principal investigator: Alain Manceau, Advanced Light Source, Ernest Orlando Lawrence Berkeley National Laboratory. Email: [acmanceau@lbl.gov](mailto:acmanceau@lbl.gov). Telephone: 510-643-2324.